# Numerical study of heat and mass transfer of a wall containing micro-encapsulated phase change concrete (PCC)

**Nour Iajimi** ( nourlajimi@yahoo.fr )
Université de Monastir
**Noureddine Boukadida**
Université de Sousse

**Research Article**

**Keywords:** phase change concrete, climatic conditions, ceiling wall

**Posted Date:** September 24th, 2021

**DOI:** https://doi.org/10.21203/rs.3.rs-305948/v2

# Numerical study of heat and mass transfer of a wall containing micro-encapsulated phase change concrete (PCC)

Nour Lajimi*, and Noureddine Boukadida[2]

[1] Ecole Nationale d'Ingénieurs de Monastir, Laboratoire de Métrologie et des Systèmes Energétiques, Université de Monastir, Rue Ibn El Jazzar, Monastir5000, Tunisia
* Correspondence:; nourlajimi@yahoo.fr;
[2] Ecole Supérieure des Sciences et de Technologie de Hammam Sousse, Laboratoire de Métrologie et des Systèmes Energétiques (Monastir), Université de Sousse, Rue Lamine Abassi, Sousse4011, Tunisia;nournour.boukadida@gmail.com

## Abstract :

The aim of this work is to study the one-dimensional heat and mass transfer through a ceiling wall containing micro-encapsulated PCC (phase change concrete) under realistic climatic conditions based on meteorological data in Tunisia based on software EnergyPlus. This work deals with a numerical study based on the nodal method to predict the effect of integration of a layer of PCC on the thermal, mass behavior and on the thermal sensation of the occupant as well as on the reduction of the energy consumption for the summer and winter period associated with the composite envelope building.

## Introduction

To improve the thermal inertia of a building envelope, we have studied another technique which is the integration of phase change concrete (PCC) thanks to the high latent heat that it exchanges during heat transfers. We note that several studies have been carried out with the aim of improving the energy performance of buildings. Laurie et al [1] used Comsol Multiphysics software to study the model of hollow core slabs serving as a floor or ceiling filled with MCP in order to increase the thermal inertia of a building. To avoid the possibility of PCM (phase change material) leaks when it is in the liquid state, a polymer / MCP composite is made and then incorporated inside the existing cylindrical cavities in the slabs of floors or ceilings. They used commercial paraffin as a PCM with a melting temperature close to 27 ° C, its apparent latent heat is around 110 KJ / kg. Then, they carried out several dynamic tests, a periodic temperature variation (between 22 and 35 ° C) was imposed on the inside face of a slab and the temperature on the upper face was measured and compared to that observed for a reference panel without MCP. They showed that the variations of this temperature have a lower amplitude when the slab contains an MCP and moreover the phase shift between the imposed variations and those measured on the other face is about 1.5 times greater for the slabs with MCP. which clearly shows the increase in thermal inertia. Sharma et al [2] have shown that the MCP microencapsulation method is best suited to the building envelope because PCMs are easy to handle and integrate into all building materials. Alexander M. Thiele et al [3] studied the addition of micro-encapsulated MCP to the exterior concrete walls of a mid-size family residence in San Francisco and Los Angeles. They used numerical simulations to process this study. The results showed that adding PCM can lead to significant annual energy savings. In fact, the annual reduction in cooling load varies from 85% to 100% and from 53% to 82% in San Francisco and Los Angeles, respectively, thus the decrease in power consumption. Jiawei Lei et al [4] numerically studied the energy performance of buildings integrating MCP in order to reduce the cooling load in

Singapore. They incorporated a 10mm thick MCP layer with a melting temperature of 28 ° C in all vertical walls either on the exterior surfaces or on the interior surfaces of the building envelope. They have shown that the optimum phase change temperature is affected by the location of the MCP and that the integration of MCP into the exterior surfaces of the walls improves the thermal performance of a building more than that of the interior surfaces. . K. Saafi and N. Daoues [5] have shown that MCP applied to the exterior face of a brick wall provides better energy efficiency, with the highest energy savings of up to 13.4% achieved for south orientation. The integration of the 3cm thick MCP improved the thermal inertia of the wall with a 2 hour increase in the jet lag for the east orientation. A 30 year life cycle cost analysis has shown that integrating MCP into a brick wall is not cost effective. The interaction between MCP and thermal insulation in a brick wall showed improved efficiency of MCP in the absence of insulation, providing the highest rate of reduction in energy consumption, estimated at 12.21 %. Integrating the MCP into the ceiling compensated for winter penalties and reduced the surface temperature to 5.35 ° C. Baniassadi et al [6] have shown that PCM is the most favorable thermal insulation in the Iranian climate. Ye et al [7] studied the comparison between PCM and thermal insulation and proved that PCM performance is better during the cooling season. Pisello et al. [8] proved that adding PCM to the ceiling minimizes energy consumption during the cooling and heating periods of Italy. Roman et al. [9] for seven climatic zones in the United States, where the PCM roof type performed better than the Cool Roof technology. Aguilar et al. [10] showed an optimal analysis of a PCM in the temperate climate of Sydney and investigated the similar influence of roof solar reflectivity and PCM on energy savings in several cases. Li et al. [11] numerically studied the thermal performance of roofs with and without PCM in China and showed that PCM increased the temperature delay through the roof by 3 h. According to Saffari et al. [12], the combination of cool roof and PCM technologies reduced roof cooling stress by 18% to 30% and resulted in energy savings of 1% to 6%.

Controlling indoor air humidity is a major factor in improving comfort in a building. N. Subramanyam et al [13] have shown that maintaining indoor relative humidity is important for improving indoor air quality, energy performance and the durability of the building envelope. [14, 15] pointed out that a low humidity environment causes dryness of the skin and throat, mucous membranes, while a high humidity environment can lead to dryness, discomfort and respiratory allergies affecting the visibility of air quality, causing fungal growth, affecting the durability of the building, etc. Shi et al. [16] concluded that PCM models are thermally efficient and that by reducing relative humidity 8% to 16%, they provide a comfortable and healthy indoor environment. Additionally, they showed that the application of PCM in social housing in Hong Kong is economically visible with an 11-year payback period. Therefore, thermal and water performance are essential for a comfortable and healthy life. For the above reasons, this research also investigated the effect of microencapsulated concrete on changes in temperature and humidity based on physical models [17,18] to predict the coupling between the transfer of heat and mass of different types of envelopes in the building. Based on the nodal method as a numerical method, we cut the building into several elements so that we got 81 nodes in total and we solved the problem of heat transfer and mass using the method of the thermoelectric analogy (Figure 1). The simplicity of the model used, based on the thermoelectricity method and validated with an analytical method [19,20], facilitated the prediction and evaluation of the energy benefits of walls and results in BC composite materials.

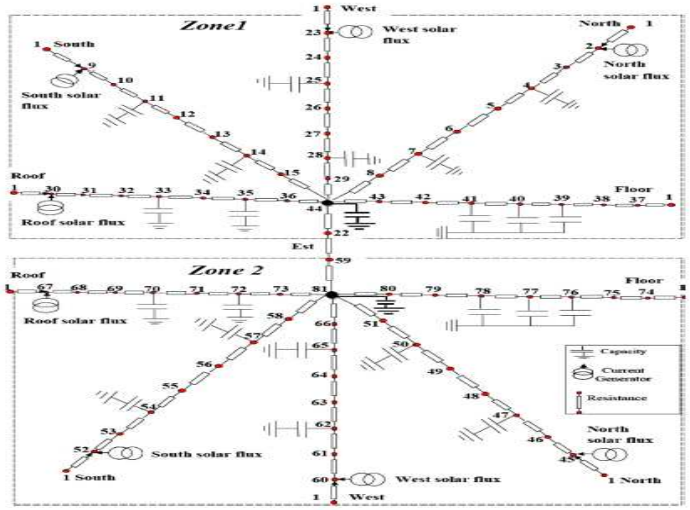


Fig.1 Thermoelectricity analogy model used for two-zone building.

## 1. Problem position

We have studied the evaluation of the hydrothermal response of micro-encapsulated PCC composite panels whose melting temperature is set to be equal to 26 ° C of a two-zone building (fig. 1) in which the walls of two zones (zone 1, zone 2) are identical (surface S = 100 $m^2$ with a height of 3m) and the effect of adding PCC in an exposed wall in the ceiling as shown in figure (2,3).

-The vertical walls which are placed on the North, South and West exposed walls are composed of:

Thin plaster and layers of plaster, brick (8 cm, 12 cm) separated by a layer of wool (5 cm)

-The ceiling is composed of a PCC layer of a thickness 3cm [5] placed on the exterior side, a layer of brick of 10 cm and a layer of concrete of 12cm (figure 2). For all the thermo-physical properties of the different layers are shown in in table1.

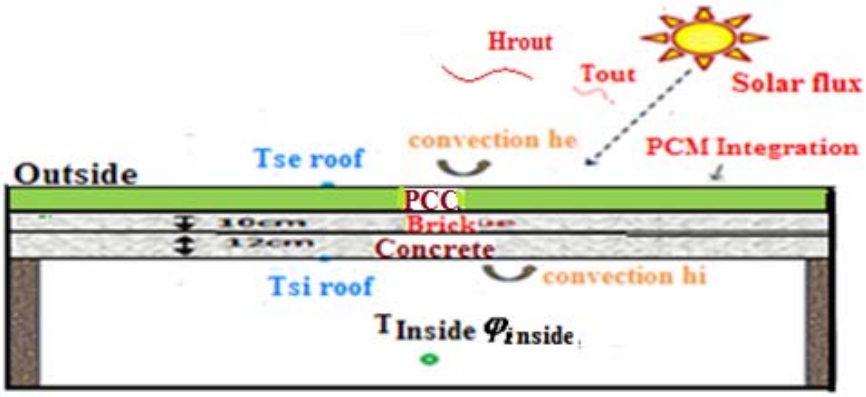


Fig.2 Integration of a layer of PCC in a wall exposed to the ceiling

-Case 1: PCC wall with a layer of 3cm thickness,

-Case 2: A wall with an insulating layer (glass wool).

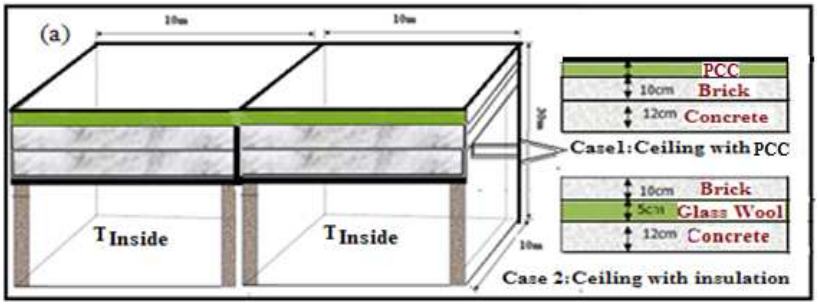


Fig3. The different cases of a multi-layered wall in a room

The thermal properties of the materials are given in the following table:

| **materials** | **thermal properties of the materials** | | |
|---|---|---|---|
| | $\rho$ (kg/m$^3$) | $c_p$ (J/kg K) | K (W/m K) |
| PCM (paraffin RT27) | 767 | 2100 | 0.185 |
| Concrete | 2300 | 880 | 1.4 |
| Brick | 1820 | 840 | 0.69 |
| coated | 1900 | 1000 | 0.93 |
| plaster | 1150 | 1000 | 0.75 |
| Glass wool | 18 | 450 | 0.039 |

Table 1 Thermo-physical properties of materials [16,17]

The heat transfer by conduction through a wall, in the case without a heat source, is described by:

$$\rho c_p \frac{dT}{dt} = k \frac{d^2T}{dx^2}$$

where ρ, cp and k are the density, thermal conductivity and specific heat capacity of the material, respectively. Modified PCM / concrete materials can be considered as two-phase materials consisting of reference concrete and PCM particles. In this case, the thermal conductivity of the composite material can be predicted from homogenization schemes as a function of the thermal conductivities of the two phases (concrete and PCM) and of their volume fractions. The expression of the effective thermal conductivity of the composite wall has been accurately predicted by Felske's model [18]:

$$k_{eff} = \frac{2k_m(1-\phi_c-\phi_s)(3+2\frac{\phi_s}{\phi_c}+\frac{\phi_s k_c}{\phi_c k_s})+(1+2\phi_c+2\phi_s)[(3+\frac{\phi_s}{\phi_c})k_c+2\frac{\phi_s k_s}{\phi_c}]}{(2+\phi_s+\phi_c)(3+2\frac{\phi_s}{\phi_c}+\frac{\phi_s k_c}{\phi_c k_s})+(1-\phi_c-\phi_s)[(3+\frac{\phi_s}{\phi_c})\frac{k_c}{k_m}+2\frac{\phi_s k_s}{\phi_c k_m}]}$$

The effective volumetric heat capacity is given by [19]:

$$(\rho c_p)_{eff}(T)=\phi_c(\rho c_p)_c(T)+\phi_s(\rho c_p)_s+(1-\phi_c-\phi_s)(\rho c_p)_m$$

It depends on the temperature, as it is written below

$$(\rho c_p)_{eff}(T)=\begin{cases}(\rho c_p)_{eff,s} & \text{for } T<T_{pc}-\Delta T_{pc}/2\\ (\rho c_p)_{eff,s}+\phi_c\dfrac{\rho_{c,s}h_{sf}}{\Delta T_{pc}} & \text{for } T_{pc}-\Delta T_{pc}/2\le T\le T_{pc}+\Delta T_{pc}/2\\ (\rho c_p)_{eff,l} & \text{for } T>T_{pc}+\Delta T_{pc}/2\end{cases}$$

## 2. Hypothesis

In this work, we have assumed the following assumptions:

-The heat and mass transfer is unidirectional.

-Air is considered a perfect transparent gas.

-The thermo-physical properties of each material are constants.

-The liquid vapor interface is permeable only to water vapor,

-Relative humidity was chosen as the potential governing mass transfer,

- The diffusion of water vapor in the air, assuming that humid air is an ideal gas, is described according to Fick's law,

-The adsorbed water remains immobile because of the strong adhesion with the pore surface

-Constant pressure

-The transfer of water vapor diffusion in building materials is expressed by the experimental correlation of Milos J. and Robert C [25]: $D=\dfrac{D_{v0}}{R_d}$

-Dv0 is the diffusion coefficient of water vapor in the air, Rd is the factor of resistance to vapor diffusion and D is the coefficient of water vapor diffusion in building materials.

• The participation energy of the occupant is taken into account. To give more precision in our calculation, we considered that the bi-zone building is occupied by two persons at rest and taking a standing position (one in the center of each zone), so breathing contributes only with 10% to the global exchange, conduction with only 1 % (given the very small contact surface of the feet with the ground [26]). These two contributions are neglected. The metabolism is assumed to be equal to 70 W.m$^{-2}$ [27].

## 3.Mathematical model:

### 3-1 balance equation

The mathematical model based on the balance equation is written:

$$(mc)_i\frac{dT_i}{dt}=\sum_{j=1,n}C_{i,j}(T_j-T_i)+\sum_{j=1,n}K_{i,j}(T_j^4-T_i^4)+P_i(t)+S(t)+L_v\,\rho\,V_i\frac{d\varphi_i}{dt}$$

Knowing that the mass balance is written [18]:

$$(Cm\ \ V)_i\frac{d\varphi_i}{dt}=\sum_{j=1,n}W_{i,j}(\varphi_j-\varphi_i)+\sum_{j=1,n}W'_{i,j}(T_j-T_i)$$

Avec:

$*(mc)_i$, $T_i$ et, $C_{i,j}$, $P_i(t)$ are the specific heat capacity, the temperature in real time, the coefficient of conductivity or convection between nodes i and j, the solar flux absorbed at time t by node i, respectively. Ki, j is the radiative coupling coefficient between i and j.

$*\varphi_i$ : relative humidity of element i

$V_i[m^3]$ : The volume of element i

$W_{i,j} = \pi.Pvs \quad [Kg.m^{-1}.s^{-1}], \quad W'_{i,j} = \pi.\varphi\frac{\partial P_{vs}}{\partial T} \quad [Kg.m^{-1}.s^{-1}.K^{-1}]$, Include the transfer of diffusion vapeur of water or convective mass transfer [17]

$Pvs = 611.213\exp\left(\frac{17.5043T}{241.2+T}\right)$: The saturated vapor pressure

$\pi$ : vapor permeability [s]

Cm : Mass capacity of the material [kg.m$^{-3}$]

Lv : Latent heat of vaporization [J.kg$^{-1}$]

* S(t) is the thermal load of the human body which is written as follows [28,29] :

$$S(t) = M - (E_{vap} + R + C)$$

Thermal exchanges by evaporation ( $E_{vap}$), radiation ( $R$ ) and convection ( $C$ ) are described by the following expressions [30] :

• $E_{vap} = h_m(P_{vs}(T_{sk}) - P_v)$ , $h_m$ (W/Pa.m²) is the evaporation coefficient. It is determined by relating it to the convective heat transfer coefficient by the Lewis ratio LR (ratio between mass transfer coefficient $h_m$ and heat transfer coefficient $h_c$ :

$LR = \frac{h_m}{h_c} = 16.5K / kPa$ (for typical indoor conditions [31]).

• $R = F_{eff}\varepsilon_{sk}\sigma(T_{sk}^4 - T_{MR}^4)$, the effective radiation area factor (a purely geometric factor) is taken for a standing person $F_{eff} = 0,725$ , and the emissivity of the skin is close to 1.

• $C = h_c(T_{sk} - T_a)$, the coefficient $h_c$ depends on the air velocity ($V_a$) of the fluid (air) and it is obtained by one of the different formulas proposed by the authors $h_c = 10V_a^{0,5}$ .

One method is to count the percentage of people dissatisfied with the comfort conditions. This percentage is directly linked to the average vote of a given population.

There are thus two parameters making it possible to measure thermal comfort:

PMV: Average Predicted Vote and is used to quantify the feeling of comfort using the standardized scale according to EN ISO 7730[32].

The Fanger equation [32] is given below:

$$PMV = \left(0.303e^{-0.036M} + 0.028\right)\left\{\begin{array}{l}(M-W)\\ -3.05\times10^{-3}\times[5733-6.99(M-W)-p_a]-0.42[(M-W)-58.15]\\ -1.7\times10^{-5}M(5867-p_a)\\ -0.0014M(34-T_a)\\ -3.96\times10^{-8}f_{cl}[(T_{cl}+273)^4-(T_{rm}+273)^4]\\ -f_{cl}h_c(T_{cl}-T_a)\end{array}\right\}$$

PPD predicts the percentage of unsatisfied people in a thermal environment [32]:

$$PPD = 100 - 95\,e^{-(0.03353PMV^4 + 0.2179PMV^2)}$$

### 3.2. Boundary and Initial Conditions

The values of the meteorological temperature and the relative humidity of the outside air are provided by the local meteorological station of Sousse as shown in figures 4.5 represent evolution of the temperature and relative humidity of the outside air according to time [19] for the months January and July and curve 6 shows the variation in the density of the incident solar flux on the exterior face of the ceiling for the months January (fig6.a) and July

(fig6.b) [19]. Direct and diffuse solar density fluxes are calculated hourly on the 15th day, which is considered a typical day of the month.

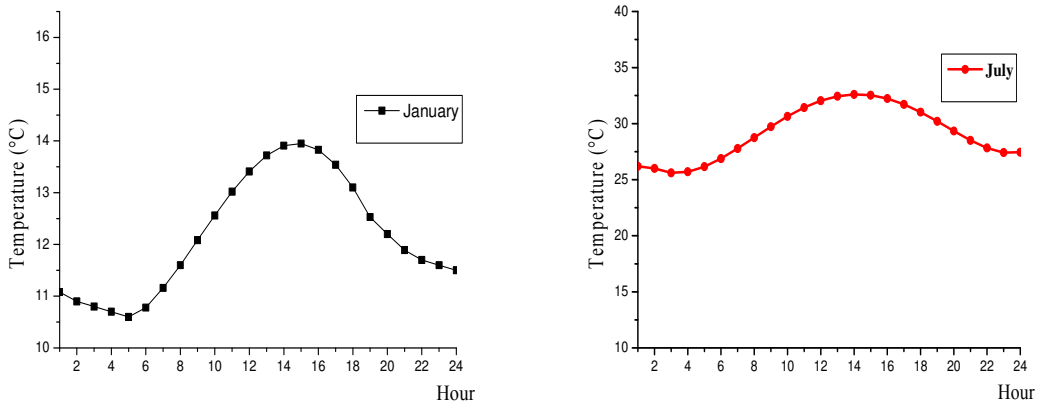


Fig.4 Hourly evolution of outdoor temperatures for the months January and July

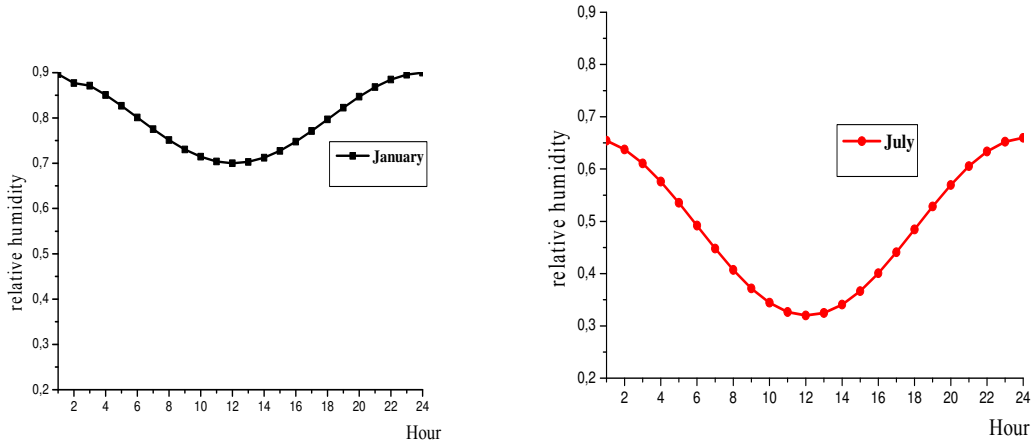


Fig5 time evolution of the relative humidity of the outside air for the months January and July

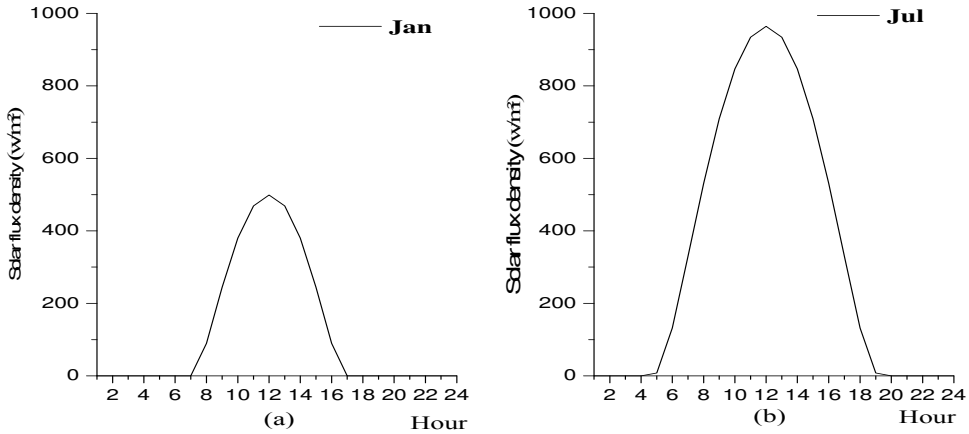


Fig.6 Time evolution of the solar flux density on the ceiling for the months of January and July.

The average emission and absorption coefficients of the exterior and interior surfaces of each wall are set respectively at ε = 0,9 et α = 0, 8.
The coefficient of heat transfer by convection at the outer and inner surfaces of the horizontal wall is he = 14[W / $m^2$K] et hi (T) en [W / $m^2$K], respectively.

## 4-Result and interpretation

- ***Evolution of thermal power (Pt) and mass (Pm) for the months January and July***

First, we have plotted the variation in thermal power (Pt) and mass (Pm) for the months January and July. We notice that there are two time intervals during a day (winter or summer):

- From 1 a.m. to 3 p.m.: there is a thermal storage which is the origin of the increase in the temperature of the indoor air (which was shown in figure 7) and a mass de-stocking which leads to the decrease in the amount of water vapor in indoor air, therefore a decrease in Hr.
- From 3 p.m. to midnight: there is a thermal destocking which is the origin of the decrease in the temperature of the interior air (which was shown in figure 7) and a mass storage which leads to the increase in the quantity of water vapor in indoor air, hence an increase in Hr.

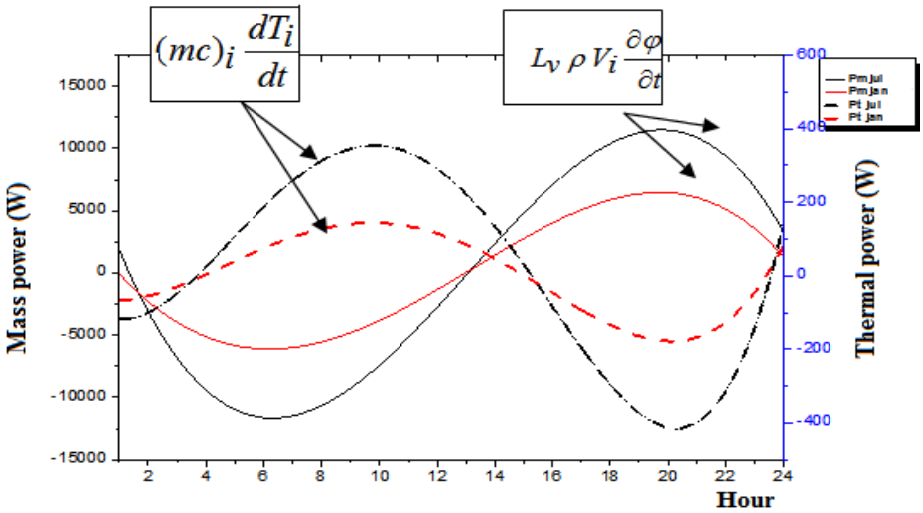


Fig7. Time evolution of thermal power (Pt) and mass (Pm) for the months January and July

***-Influence of the nature of a multilayer wall on the temperature and humidity of the indoor air.***

-We have plotted the evolution of the temperature of the interior air according to the different cases of the multilayer walls for the months July (fig. 8) and January (fig. 9). We have observed that the integration of the PCC during the summer period allows to reduce the temperature of the indoor air compared with a wall provided with a layer of glass wool. The difference between the room temperature without PCC and that of the room with PCC can reach 3 ° C. This is due to the large storage capacity provided by the phase change material. During the winter period, this temperature variation is small, around 1 ° C. We have traced the evolution of the relative humidity of the indoor air (fig. 10,11) of a wall with PCC and wall with glass wool for the months of January and July. We have noticed that there is a difference between the indoor air humidity of the room without PCC and that of the room with PCC, which can reach 8% during the month of January and for the month of July with a difference of 12%. It can be seen that the addition of PCC improved the reduction in relative humidity. In addition, this feature can be useful in reducing air conditioning cooling loads and hence power consumption.

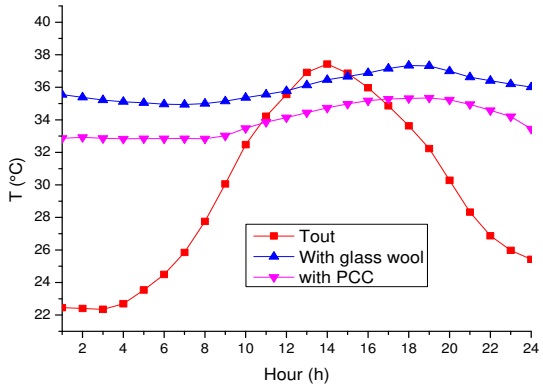


Fig.8 temperature evolution indoor air for the month of July

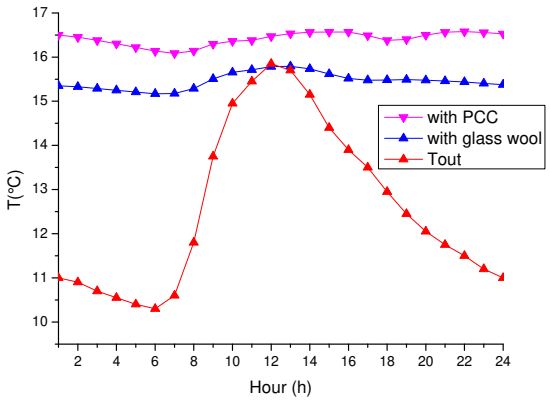


Fig.9 temperature evolution indoor air for the month of January

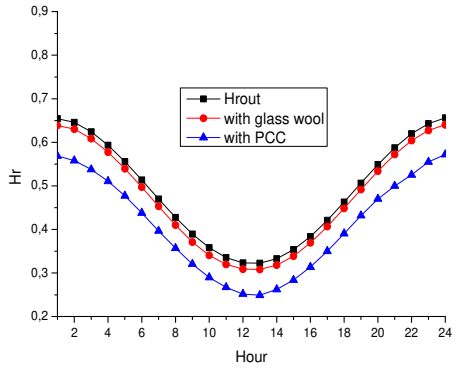


Fig.10 relative humidity evolution indoor air for the month of January

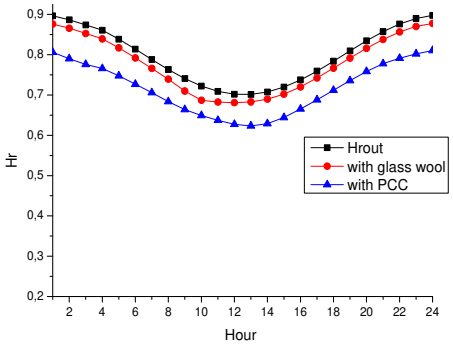


Fig.11 relative humidity evolution indoor air for the month of July

***-Impact of different types of multilayer walls on energy consumption***

the figures represent the daily evolution of the total power consumed by the indoor air for the different types of premises in the month of July (fig. 12a) in the case where the indoor air temperature is maintained at 25 ° C for all day and month of January if the indoor air temperature is set at 19 ° C throughout the day. It has been noted that the average air conditioning power consumed by the indoor air (fig 12.a) is around 5426 W for a room with glass wool and 4001 W for a room with PCC. This difference is due to the role of the PCC which ensures the increase in the thermal inertia of the building. We can then say that a room with PCC consumes less energy than a room with glass wool of around 14%. In the case of heating (fig. 12b) The average powers consumed for the two cases are appreciably similar and they are of the order of 1051 W for the room (glass wool), of 963 W for the room (with PCC) . They are more important during the night period than the daytime period. For the room (with PCC), during the night time the energy consumption is lower than that for a room (glass wool), thanks to the importance of the heat capacity which this room has to store heat during the period of sunshine (room with high inertia). During the daytime consumption is slightly higher than that of the local with glass wool, this is due to the accumulation of latent heat which ensures a large amount of energy stored during the day and large energy consumption. We have observed that the energy consumption in the case of an air conditioning application (month of July) is high with a reduction rate of 35% than that in the case of an application of type of heating (month of January) with a rate of 15% (fig 13) and that due to the influence of the solar flux (see figure 4).

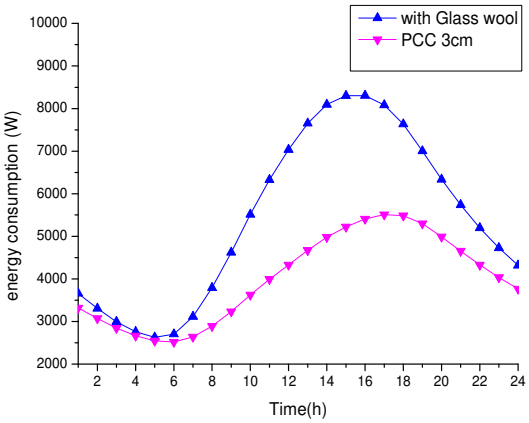


Fig.12a during the month July

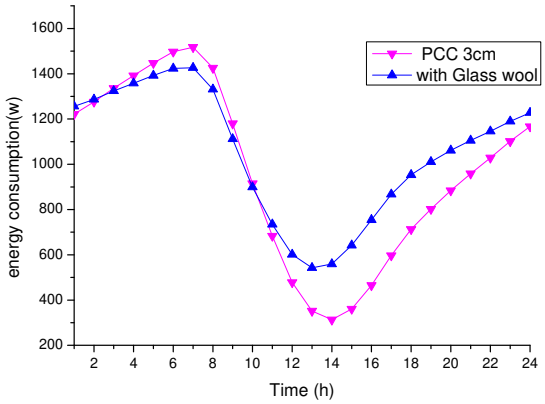


Fig.12b during the month January

Fig.12 Time evolution of energy consumption

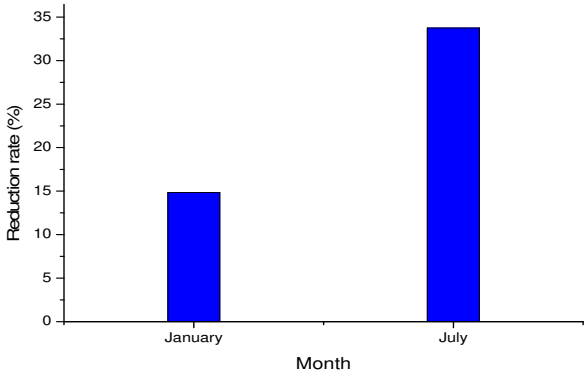


Fig.13. The variation in the reduction rate for the month July and for the month January

***- Influence of the nature of a multilayer wall on the thermal sensation of the occupant for the month of July***

To quantify sensation of comfort using the standardized scale according to EN ISO 7730 [32]. Figure 14 shows relationship between the percentages of dissatisfied (PPD) and the average vote (PMV) for different configurations (wit and without PCC) . We notice the thermal sensation of the occupant is tepid in the case where the ceiling with PCC, on the other hand in the case where the ceiling without PCC the thermal sensation is almost hot.

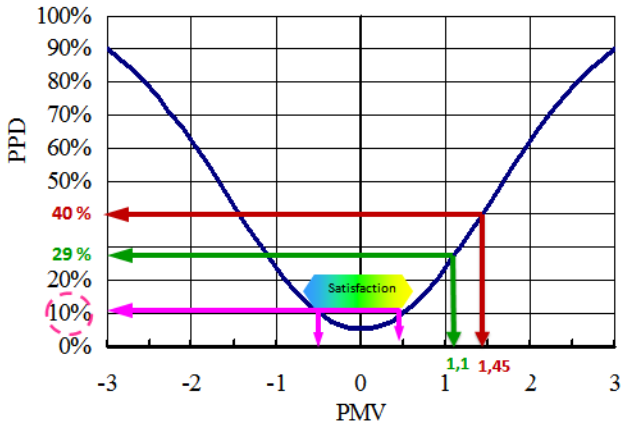


Fig. 14 Relationship between the percentages of dissatisfied (PPD) and the average vote (PMV) for different configurations

In Table 5, we plotted the comfort index for different configurations studied.

| Configuration | Without BCP | With BCP |
|---|---|---|
| PMV | 1.1 | 1.45 |
| PPD | 29% | 40% |

### *-Influence de la nature de paroi sur le cout énergétique totale.*

A thermo-economic analysis of the wall of the envelope incorporated with PCM by varying its thickness will allow us to analyze the optimization of the cost of heating or cooling during the winter and summer periods.
According to [5] the total cost per unit area of the wall Ct, including the present value of energy cost ($C_{enr}$) and PCM cost ($C_{PCM}$) is given by:

$$C_t = C_{enr} + C_{MCP} = PWF\left(\frac{Q_C}{COP}\frac{Cel}{(3.6.10^6)} + \frac{Q_h}{Hu.\eta s}C_g\right) + C_{MCP}$$

With:
- Qh and QC are the energy consumption of air conditioning and heating.

The parameters used in the economic calculations used [5] are: $Bio_{PCM}$ cost, $C_{PCM}$: 5.64 TND / $m^2$, Cost of electricity (for cooling) Cel: 0.21 TND / kWh, Coefficient of performance of the air conditioning system COP = 3, Cost of Natural gas (for heating) Cg: 0.2515 TND / m3, The calorific value, Hu = 34.526 106 J/m3 and Efficiency of the heating system $\eta_S = 0.8$
PWF: the present value Factor which is an economic indicator defined as:

$$PWF = \sum_{u=1}^{n}\frac{(1+i)^{u-1}}{(1+d)^u} = \begin{cases}\frac{1}{d-i}\left[1-\left(\frac{1+i}{1+d}\right)^n\right] & i \neq d \\ \frac{n}{1+i} & i = d\end{cases}$$

i: The inflation rate is 5.5%,
d: The discount rate is 7%
This table shows the total energy cost during the winter and summer periods by varying the nature of the wall of a room. We have noticed that there is a reduction in cost of 20%.

| Nature of the Wall | A layer of glass wool | A layer of PCC |
|---|---|---|
| Energy cost (TND/m²) | 95.05 | 75.07 |

Table 2 the total energy cost during winter and summer periods

## Conclusion:

In this work we studied the effectiveness of the integration of PCC in the ceiling of a Tunisian building; especially in terms of energy savings where heating and cooling have become essential. The results obtained show in particular that:
- The temperature of the inner surface of the PCC wall is slightly reduced compared to glass wool insulation.
- The percentage reduction in the relative humidity for the PCC wall is around 8% for the month of January and 12% for the month of July. In addition, this feature can be useful to reduce air conditioning cooling loads and therefore energy consumption.
-The thermal sensation of the occupant is tepid in the case where the ceiling with PCC
-An economic analysis has shown that the use of PCC reduces the energy cost by 20%.

### Bibliography reference

**[1]Laurie** et al (2013) Amélioration du confort thermique par intégration de MCP dans les planchers/plafonds de bâtiment à structure légère ", 16ème Journées Internationales de thermique

**[2]Sharma, A, V.V, Tyagi, C.R, Chen et D, Buddhi**(2009). Review on Thermal energy storage with phase change materials and Applications.Renewable and Sustainable energy reviews. Vol. B, page 318-345

**[3]Alexander M. Thiele** et al (2015) Diurnal thermal analysis of microencapsulated PCM/concrete walls, Energy Convers. Manag. Volume 93, pp. 215–227.

**[4]Jiawei Lei** et al (2016) "Energy performance of Building envelopes integrated with phase change materials for cooling load reduction in tropical Singapore", Nanyang Technological University, Applied Energy volume 162, pp. 207-217.

**[5]K. Saafi** , **N.Daoues** (2019) Energy and cost efficiency of phase change materials integrated in building envelopes under Tunisia Mediterranean climate, Energy volume 187.

**[6]Baniassadi A, Sajadi B, Amidpour M, Noori N**. Economic optimization of PCM and insulation layer thickness in residential buildings. Sustain Energy Technol Assess 2016;14:92e9. https://doi.org/10.1016/j.seta.2016.01.008.

**[7]Ye H, Long L, Zhang H, Zou R**. The performance evaluation of shape-stabilized phase change materials in building applications using energy saving index. Appl Energy 2014;113:1118e26. https://doi.org/10.1016/j.apenergy.2013.08. 067.

**[8] Pisello AL, Castaldo VL, Cotana F**. Dynamic thermal-energy performance analysis of a prototype building with integrated phase change materials. Energy Procedia 2015;81:82e8. https://doi.org/10.1016/j.egypro.2015.12.062.

**[9] Roman KK, O'Brien T, Alvey JB, Woo OJ**. Simulating the effects of cool roof and PCM (Phase Change Materials) based roof to mitigate UHI (Urban Heat Island) in prominent US cities. Energy 2016;96:103e17. https://doi.org/10.1016/j. energy.2015.11.082.

**[10] Aguilar JLC, Smith GB, Gentle AR, Chen D**. Optimum integration of albedo, subroof R-value, and phase change material for cool roofs. In: 13th conference of international building performance simulation association, chambery-France; 2013.

**[11] Li D, Zheng Y, Liu C, Wu G**. Numerical analysis on thermal performance of roof contained PCM of a single residential building. Energy Convers Manag 2015;100:147e56. https://doi.org/10.1016/j.enconman.2015.05.014.

**[12] Saffari M, Piselli C, de Gracia A, Pisello AL, Cotana F, Cabeza LF**. Thermal stress reduction in cool roof membranes using phase change materials (PCM). Energy Build 2018;158:1097e105. https://doi.org/10.1016/j.enbuild.2017.10. 068.

**[13] N. Subramanyam, M.P. Maiya, S.S. Murthy**, Application of desiccant wheel to control humidity in air-conditioning systems, Applied Thermal Engineering, 24 (17–18) (2004) 2777-2788.

**[14] Z. Rao, S. Wang, Z. Zhang**, Energy saving latent heat storage and environmental friendly humidity-controlled materials for indoor climate, Renewable and Sustainable Energy Reviews, 16 (5) (2012) 3136-3145.

**[15] H. Zhang, H. Yoshino**, Analysis of indoor humidity environment in Chinese residential buildings, Building and Environment, 45 (10) (2010) 2132-2140.

**[16]X Shi, SA Memon, WC Tang, HZ Cui, F Xing**. Experimental assessment of position of macro encapsulated phase change material in concrete walls on indoor temperatures and humidity levels. Energy Build 71 (2014) 80–7

**[17]S.Dubois** et al (2014) Non-isothermal moisture balance equation in porous media: a review of mathematical formulations in Building Physics, Biotechnol. Agron. Soc. Environ. volume 18,pp. 383-396

**[18]F. Tariku** et al (2010)Transient model for coupled heat, air and moisture transfer through multilayered porous media. International Journal of Heat and Mass Transfer, volume 53 pp.3035–3044

**[19]Lajimi N., Boukadida N**. (2015) "Numerical study of the thermal behavior of bi-zone buildings", Comptes Rendus Physique Volume 16, issue, 8, pp. 708–720.

**[20]N.Bentaher** et **Lajimi N.** (2019) Evaluation of the effect of a phase-change material on the thermal response of a bizone building under the climatic conditions of Tunisia C. R. Physique Elsevier volume 20 ,pp.593–603

**[21] Biwole, P.** et al (2013) Phase-change materials to improve solar panel's performance. Energy and Buildings, 62, 59–67.

**[22]Incropera FP,** et al., “Fundamentals of heat and mass transfer”, New York City: John Wiley & Sons; 2011.

**[23] JD Felske** Effective thermal conductivity of composite spheres in a continuous medium with contact resistance. International Journal of Heat and Mass Transfer, 2004 - Elsevier.pp.3459-3461

**[24]Alexander M.Thiele** et al (2015)Annual energy analysis of concrete containing phase change materials for building envelopes, Energy Conversion and Management, Volume 103, pp. 374-386

**[25]**Milos J., Robert C. (2012). Effect of moisture content on heat and moisture transport and storage properties of thermal insulation materials Energy and Buildings 53, pp. 39–46.

**[26]** Françoise Thellier. Modélisation du comportement thermique de l'homme et de son habitat. Une approche de l'étude de confort, thesis, Thermics. Université Paul Sabatier - Toulouse III, 1989.

**[27]** Serres. L, Trombe.A, and Miriel. J, Flux solaires absorbés par l'occupant d'un local vitré. Prise en compte dans l'équation du confort thermique, *Int. J. Therm. Sci.* 40, (2001), pp. 478–488.

**[28]**. Lee, S. et al, Field thermal performance of naturally ventilated solar roof with PCM heat sink. Solar Energy, 86, (2009), pp.2504-2514.

**[29].** Moujalled. B, Modélisation dynamique du confort thermique dans les bâtiments naturellement ventilés, thesis. N° d’ordre 2007-ISAL-0005, Ecole Nationale des Tavaux Publics de l’Etat, Lyon, 2007.

**[30**]. Françoise Thellier. Modélisation du comportement thermique de l'homme et de son habitat. Une approche de l'étude de confort, thesis, Thermics. Université Paul Sabatier - Toulouse III, 1989.

**[31].** Conrad Voelker et al, Heat and moisture transfer through clothing, Eleventh International IBPSA Conference Glasgow, Scotland July 27-30, 2009.

[32] EN ISO 7730, Moderate thermal environments. Determination of PMV and PPD indices and specifications of thermal comfort conditions. ISO, Genève, et CEN, Bruxelles1994